BIOCHEMISTRY
including biophysical chemistry & molecular biology

Article

pubs.acs.org/biochemistry

Intermediates Stabilized by Tryptophan Pairs Exist in Trpzip Beta-Hairpins

Zhongbo Yu,[#] Sangeetha Selvam, and Hanbin Mao*

Department of Chemistry and Biochemistry, Kent State University, Kent, Ohio 44242, United States

Supporting Information

ABSTRACT: Transitions of protein secondary structures, such as alpha-helices and beta-hairpins, are often too small and too fast to follow by many single-molecular approaches. Here we describe new population deconvolution methods to investigate the mechanical unfolding/refolding events in Trpzip β-hairpins that are tethered between two optically trapped polystyrene particles through click chemistry. The application of force to the Trpzip peptides shifted population distribution, which allowed us to identify intermediates from regular force−extension curves of the peptides after population deconvolution analysis. Comparison of the intermediates between the Trpzip2 and Trpzip4 peptides suggests the intermediates are likely stabilized by the tryptophan pair stacking. We anticipate the method of population deconvolution described here can offer a unique capability to investigate fast transitions in small biological structures.

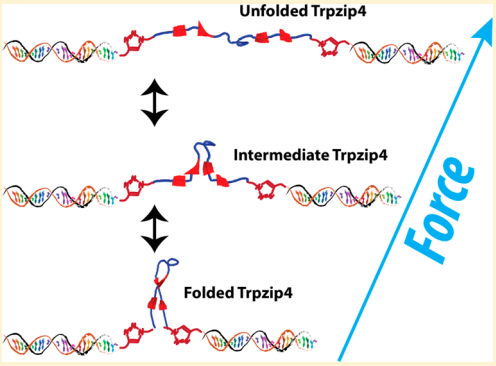

Mechanism of protein folding and unfolding provides fundamental understanding on protein functions in cells, which include nascent protein synthesis, protein−protein or protein−ligand interactions, and enzyme dynamics. Exploration of protein folding principles has led to broad applications in pharmacology,[1,2] medicine,[3,4] and biological engineering.[5−7] Using folding principles, de novo proteins have been designed to present desirable properties for materials and medical applications.[8] After decades of intensive research, many protein folding mechanisms have been proposed. For example, the kinetic partitioning mechanism[9] describes that an unfolded protein follows multiple pathways to reach its native folding conformation. Except for the two-state folding pathway, the formation of at least one intermediate is necessary in protein folding, which is characterized by a manifold of discrete local energetic minima. Among these free energy minima, it remains a technical difficulty to identify intermediates, especially for fast transitions.

Ensemble techniques such as NMR, X-ray, and circular dichroism (CD) collect signals from a large set of molecules to distill an average protein conformation or folding/unfolding dynamics. These methods are difficult to resolve the heterogeneous nature of protein transitions in the anisotropic folding or unfolding energy landscape. Single-molecule techniques entail an unprecedented resolution to address this issue. Among various single-molecule approaches, force-based techniques present three unique advantages. First, the transition dynamics of a biomolecule is overdamped[10] because of the drag force exerted on the trap-surface-handle-biomolecule system. This not only closely mimics the physiological conditions surrounding a protein secondary structure, which is tethered to large objects from its two ends, but also slows down the kinetics and benefits the analysis for intermediates. Second, proteins can be denatured by mechanical force at room temperature under physiologically relevant buffer conditions. This eliminates interference of thermal or chemical origins. Inside cells, mechanical force has been widely used to unfold and refold proteins in proteasomes and chaperones,[11−13] respectively. Compared to thermal or chemical denaturations that have a global effect on protein structures, the effect of force is local. Such a property brings the third advantage of force: it allows a desired folding or unfolding pathway along which a mechanical force is applied.[14] In fact, this capability permits the reconstruction of a full folding/unfolding energy landscape of DNA hairpins and proteins along specific directions.[15,16] Using the ergodicity principle,[9] such a landscape can be retrieved from state populations even though data acquisition rates are orders of magnitude slower than the transition rates of biomolecules.[15−17]

One particular difficulty in the protein research comes from the unstable, stand-alone secondary structures. To circumvent this problem, top-down approaches become prevalent to investigate tertiary structures of a protein, from which properties of secondary structures can then be inferred. The paucity of information on protein secondary structures has hindered the full appreciation of their roles in overall protein structures. This fact is in contrast with DNA or RNA, in which stable secondary structures such as hairpins or G-quadruplexes[15,18,19] allow thorough characterization of their properties with a bottom-up fashion.

Received: February 14, 2014
Revised: August 9, 2014
Published: August 28, 2014

dx.doi.org/10.1021/bi500194g | *Biochemistry* 2014, 53, 5978−5986

As one of the smallest peptides that can fold into a well-defined secondary conformation, β-hairpins[20−22] have become an invaluable system to elucidate folding principles of proteins.[23−27] In addition to the structural roles,[28,29] β-hairpins are important for biological processes such as fibril formation in Alzheimer and Parkinson diseases[28] and recognition of nucleic acid structures.[30,31] Limited by the spatial and temporal resolution of available mechanical unfolding approaches, however, the stand-alone secondary protein structures such as β-hairpins have not been well characterized. Here, we develop a population-based strategy to probe the intermediates of Trpzip β-hairpins (12−16 aas) by repetitive unfolding and refolding of this secondary structure with optical tweezers. By varying the external forces loaded to the β-hairpins, we shifted the folding equilibrium to favor possible intermediates. Our results reveal that Trpzip hairpins can be unfolded and refolded in a broad force range of tens of picoNewtons. A population deconvolution algorithm at nanometer resolution (PoDNano) shows a three-state unfolding pathway for the peptide through an intermediate whose size matches that of a conformation stabilized by a tryptophan pair. The three-state unfolding and refolding mechanism has not been observed experimentally in the Trpzip4 peptide.

MATERIALS AND METHODS

Unless specifically noted, DNA oligonucleotides were purchased from Integrated DNA Technologies (IDT) and PAGE purified. Enzymes and DNA plasmids were purchased from New England Biolabs (NEB). Chemicals (>99% in purity) were obtained from VWR.

Preparation of Trpzip Beta-Hairpin Constructs. We prepared two peptide−DNA constructs. One construct contains Trpzip4 peptide, GEWTWDDATKTWTWTE (>95%, Anaspec, Fremont, USA), and the other contains Trpzip2 peptide, SWTWENGKWTWK (>95%, Apeptide, Shanghai, China). Both peptides are functionalized at the N- and C-termini with propargylglycine (Scheme S1, Supporting Information). To mechanically unfold or refold Trpzip beta-hairpin structures, we sandwiched the peptide of interest using two double-stranded (ds) DNA handles. We prepared two different 2028 bp PCR handles amplified from a pBR322 template using a 5′ azide-dUTP labeled primer (IDT) and a second primer modified with either a biotin or digoxigenin at the 5′ end. These two PCR handles were mixed with the propargylglycine modified peptide at an equal molar ratio (0.5 μM) in 10 μL volume. The azide−alkyne Huisgen cycloaddition (click chemistry[32]) was initiated by adding 3 μL of freshly prepared solution (DMSO/*t*-BuOH (3:1, v/v)) that contains 33 mM CuBr and 67 mM TBTA (Tris[(1-benzyl-1*H*-1,2,3-triazol-4-yl)methyl]amine, Sigma). After the reaction mixture was incubated overnight at room temperature without light, the DNA−peptide construct was ethanol precipitated. The products of this click chemistry reaction are a mixture of the Trpzip peptide sandwiched between various PCR handles. However, during the single-molecule optical-tweezers experiments, only the construct with a biotin at one terminus and a digoxigenin at the other would be tethered between two optically trapped beads. These peptide−DNA constructs were stored in a degassed buffer (100 mM KCl and 10 mM Tris, pH 7.4) at −80 °C for future use.

To prepare a control construct containing dsDNA handles only, we used 1,6-heptadiyne (Sigma-Aldrich) instead of peptide in a reaction condition identical with that described above.

Circular Dichroism (CD). To verify whether beta-hairpin conformation was formed in the peptide modified by the two propargylglycine residues, we performed CD using a 1-mm light path cuvette in a 20 mM sodium phosphate buffer (pH 7.4) at 23 °C. Both Trpzip4 and Trpzip2 CD spectra showed signatures rather similar to those in the literature,[20,33] demonstrating that the conformation of the beta-hairpin remained the same after the propargylglycine modification (Figure S1, Supporting Information).

Single-Molecule Force-Ramp Assay. Single-molecule force-ramp assay was performed in home-built dual-trap 1064 nm laser tweezers[34−37] at 23 °C using a degassed 20 mM sodium phosphate buffer (pH 7.4). Two beads, one immobilized with the peptide construct prepared above via digoxigenin−antidigoxigenin−antibody interaction (2.10 μm bead diameter, Spherotech) and the other coated with streptavidin (1.87 μm diameter, Spherotech), were trapped by two laser foci separately. After characterizing the trap stiffness for each trapped bead, we let two beads touch against each other by moving one of the beads using a motorized steerable mirror that controls one of the laser foci. This allowed the tethering of the peptide−DNA construct between the two beads. The tethered peptide construct was extended (until 60 pN) and relaxed (to 0 pN) by moving the two trapped beads apart and together, respectively, with a load rate of 5.5 pN s^{-1}. During these processes, the force−extension (F−X) curves for the tethered molecule were recorded at 1000 Hz using a Labview program. The raw data were filtered with a Savitzky−Golay function with a specific time constant in a Matlab program.

A single dsDNA molecule undergoes denaturing transition at the characteristic force of 65 pN[38] in our laser tweezers instrument, which confirms the accuracy of force determination. In addition, single deoxynucleotide length is measured in our laser tweezers instrument to verify the accuracy of the distance measurement. As described in the literature,[39] a dumbbell force-ramp assay was designed to mechanically unfold a single-stranded DNA hairpin with a tetrathymine loop (underscored), 5′-GC $(T)_{10}$ GC TTTT GC $(A)_{10}$ GC-3′. Extensible worm-like-chain (WLC) function[38] was used to fit the resulting F-X curves in a sequential fashion,[39] which describes a segment of the ssDNA hairpin and a segment of dsDNA handles in the molecule construct. We obtained the single deoxynucleotide contour length of 0.44 ± 0.02 nm (mean ± std), which agrees well with that measured by Block and co-workers[15] and within the range for those obtained by others.[40−43] The contour length measurement of single amino acid discussed in the main text is 0.35 nm, which falls in the range of 0.34−0.40 nm per amino acid in the literature.[44−52] This again verifies the accuracy of spatial measurement of our instrument.

Plot of Change in Contour Length vs Force (ΔL-F). For each F-X plot, we separated the stretching region and the relaxing region. At a particular force, we subtracted the extension during the stretching process from that during the relaxing process, which resulted in a plot of force vs change in extension (Δx). In Figures 1C, 2A, 3A, and 4A, the Δx was converted to the change in contour length (ΔL) at a particular force using the WLC model (eq 1)[53] on the assumption that the peptide sequence has a negligible length compared to those of the dsDNA handles (<5%):[37]

dx.doi.org/10.1021/bi500194g | *Biochemistry* 2014, 53, 5978−5986

$$F = \left(\frac{k_B T}{P_D}\right)\left[\frac{1}{4(1 - x/L_0 + F/S_D)^2} - \frac{1}{4} + \frac{x}{L_0} - \frac{F}{S_D}\right] \quad (1)$$

where x is the end-to-end distance (or extension) between the two beads, k_B is the Boltzmann constant, T is absolute temperature, L_0 is the contour length, S_D is the stretching modulus (1226 pN[54]), and P_D is the persistent length (51.95 nm[54]) for double-stranded DNA. This method allowed a straightforward approach to retrieve ΔL and rupture force for folded biomolecular structures.

Population Deconvolution with Nanometer Resolution (PoDNano). Overlapped ΔL–F traces present a large set of ΔL data in a particular force range. To identify the number of Gaussian peaks in the ΔL populations (Figure 2B, 3B, and Figure S2, Supporting Information), we iteratively fit the ΔL histogram by increasing the number of Gaussian components. Next, we compared the fitting to the original distribution by running a penalized Chi-square (χ^2) analysis. χ^2 is defined as $\sum_i((y - y_i)/\sigma_i)^2$, where y is fitted value for a given point, y_i is measured data, and σ_i is an estimate of the standard deviation for y_i. We constrained the complexity of the mixed Gaussian model by adding χ^2 with a penalty term, i.e., $\chi^2 = \chi^2 + (N \ln j/2)$, where N is the number of data points and j is the total number of Gaussian components. The best fitting shows three Gaussian peaks, i.e., the penalized χ^2 reaches a minimum with three Gaussian components. The populations were also determined by bootstrapping on the original 261 overlapped ΔL–F plots with 3000 resampling steps. For each resampling, we repeated the Gaussian fitting procedure as described above and collected the information on two most probable populations. Histograms of all these identified peaks were constructed in Figures 2C,D and 3C, from which different populations can be readily identified. The PoDNano algorithm is available upon request.

Determination of Number of Amino Acids in a Conformation. To determine the exact number of amino acids involved in a conformation under our experimental conditions, we first estimated the contour length of single amino acid (L_{aas}) based on the largest ΔL measured in the ΔL–F plots. For a two-state transition (Figure S4A, Supporting Information), or the transition between the second and third states, or that between first and third states in a three-state model (Figure S4B, Supporting Information), we used the equation[46]

$$L_{aas} = (\Delta L + x)/n \quad (2)$$

where x is the end-to-end distance or handle-to-handle distance, n is the number of unfolded amino acids, L_{aas} is the contour length for single amino acid, and ΔL is the change in contour length between folded and unfolded states. We measured both Trpzip4 and Trpzip2 beta-hairpins, where ΔL equals 48 ± 3 Å and 38 ± 2 Å (mean ± std), respectively, for the transitions between fully folded to fully unfolded states. Taking x as 6.0 ± 0.4 Å and 5 ± 1 Å (mean ± std) for Trpzip4 (PDB 1LE3, distance between atom #1 and #262, $x_{atom\ 1-262}$) and Trpzip2 (PDB 1LE1, distance between atom #1 and #198, $x_{atom\ 1-198}$) beta-hairpins,[20] respectively, the estimated L_{aas} is 3.4 ± 0.5 Å and 3.6 ± 0.1 Å (mean ± std) for Trpzip4 and Trpzip2, respectively, which agrees with the literature.[55−58,44−52] We took the average of 3.5 ± 0.5 Å (mean ± std) as the L_{aas}.

Number of amino acids released during structural unfolding can be derived by rearranging eq 2, $n = (\Delta L + x)/L_{ass}$. However, two end-to-end distances should be taken into account when the transition between the first and second states in a three-state transition (Figure S4B, Supporting Information) takes place. The following calculation is used to obtain the number of amino acids released in such scenario,

$$n = (\Delta L + x_1 - x_2)/L_{aas} = (\Delta L + \Delta x)/L_{aas} \quad (3)$$

where x_1 and x_2 represent the end-to-end distances of the conformations before and after the unfolding transition, respectively. For a folding process, folded number of aas between two states can be treated in the same way.

With experimentally determined L_{aas} and x from NMR structures,[20] we used eqs 2 or 3 to calculate the number of amino acids, n, involved in a particular folding/unfolding state. For example, 2.1 and 2.8 nm of ΔL represent eight amino acids for Trpzip4 unfolding (using eq 2 and $x_{atom\ 63-173}$ = 5.5 ± 0.1 Å (mean ± std), the average distance between atom #63 and #173 from 20 PDB 1LE3 conformations) and refolding (using eq 3 and $\Delta x = x_{atom\ 1-262} - x_{atom\ 63-173}$ = 6.0−5.5 Å = 0.5 ± 0.4 Å (mean ± std)) processes, respectively (see Figure S3, Supporting Information for the origin of different ΔL values that correspond to the same intermediate during the unfolding or refolding transition). 1.6 ± 0.2 nm and 2.5 ± 0.2 nm (mean ± std) of ΔL represent around six amino acids for Trpzip2 unfolding (using eq 2 and $x_{atom\ 52-136}$ = 5.50 ± 0.08 Å (mean ± std), the average distance between atom #52 and #136 from 20 PDB 1LE1 conformations) and refolding (using eq 3 and $\Delta x = x_{atom\ 1-198} - x_{atom\ 52-136}$ = 5−5.5 Å = −0.5 ± 1 Å (mean ± std)) processes, respectively.

Deconvolution of ΔL Populations with Point-Spread Functions. Apart from the statistical PoDNano method to deconvolute the protein folding/unfolding states, a point-spread-function (PSF)[15] based strategy can also be applied. This method recovers the true ΔL populations of Trpzip peptides by taking into account the thermal fluctuations (in a form of point-spread function) from the two optically trapped beads and the dsDNA handles. To obtain PSF, we prepared a DNA construct that contains two 2028 bp dsDNA handles linked by 1,6-heptadiyne (see above). After 300 rounds of stretching and relaxing processes, ΔL–F plots were prepared as described above. PSF functions were obtained by the Gaussian fitting on the ΔL histograms at different force levels (Figure S6, Supporting Information). These PSFs were then used to deconvolute ΔL populations in each force section (Figure 4).

The deconvolution procedure employs nonlinear constrained iterative methods,[15] where the final ΔL distribution of $p(\Delta L)$ is approached from the initial distribution of $p^{(0)}(\Delta L)$ iteratively based on a particular PSF, $S(\Delta L)$,

$$p^{(k+1)}(\Delta L) = p^{(k)}(\Delta L) + r[p^{(k)}(\Delta L)] \\ (P(\Delta L) - S(\Delta L) \otimes p^{(k)}(\Delta L));$$
$$r[p^{(k)}(\Delta L)] = r_0\left(1 - 2\left|p^{(k)}(\Delta L) - \frac{1}{2}\right|\right) \quad (4)$$

where k stands for the index of the iteration. The relaxation function $r[p^{(k)}(\Delta L)]$ constrains the solution to remain within the physical boundaries with the amplitude r_0 controlling the speed of convergence. We used r_0 = 1 with 5000 iterations. We smoothed the measured ΔL probability distribution, $p(\Delta L)$, in a 0.1 nm window. The deconvolution was performed in a house-written Igor program, which will be supplied upon request.

dx.doi.org/10.1021/bi500194g | Biochemistry 2014, 53, 5978−5986

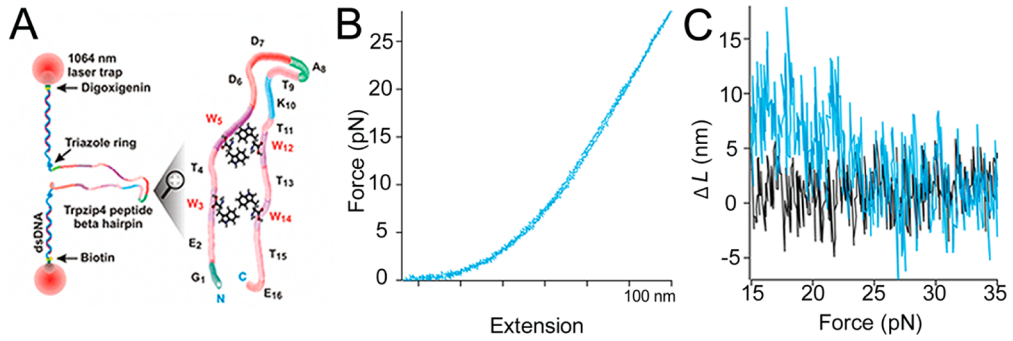

Figure 1. Unfolding of Trpzip4 beta-hairpin using dual-trap optical tweezers. (A) Schematic of mechanical manipulation (not to scale). Trpzip4 peptide is linked to dsDNA handles through triazole ring which was formed after click chemistry reaction. Dual-trap optical tweezers holds the molecule in a dumbbell fashion through affinity interactions between the molecule and polyethylene microspheres. Sequence of the Trpzip4 peptide is shown with one letter amino acids code. Tryptophan's are highlighted by ball-and-stick style. (B) Representative force–extension trace (100 Hz) for Trpzip4 construct. (C) Unfolding of Trpzip4 beta-hairpin is revealed by comparisons of ΔL-F traces (100 Hz) from the construct with Trpzip4 (blue) and that without Trpzip4 (black).

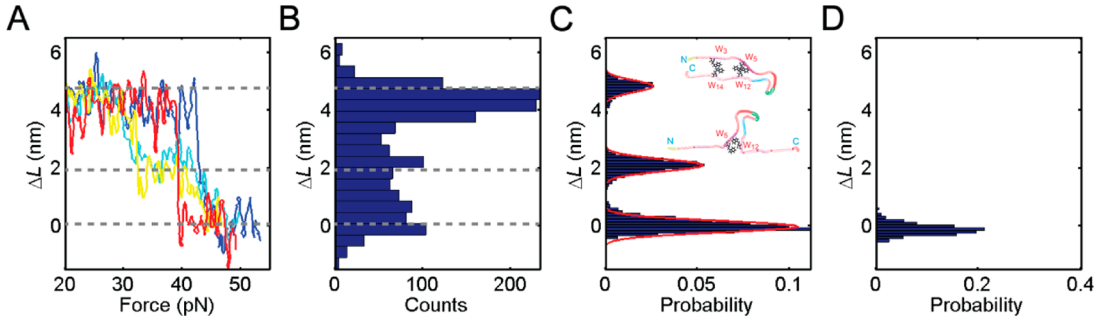

Figure 2. Trpzip4 beta-hairpin unfolds via intermediates. (A) Four representative traces of ΔL–F (20 Hz filtering) show either single (red and blue) or multiple (yellow and cyan) ΔL transitions upon force increment. (B) ΔL histogram based on the four traces in (A) reveals three populations. (C) The PoDNano method reveals three ΔL populations, which correspond to folded (top, ΔL = 4.8 nm), intermediate (middle, ΔL = 2.1 nm), and unfolded (bottom, ΔL = 0 nm) states of the Trpzip4 peptide as illustrated by cartoons (insets). Red curves represent Gaussian fittings. (D) The PoDNano analysis shows one population (ΔL = 0 nm) for a control DNA construct without Trpzip4 (see Materials and Methods). For comparison, three dashed gray lines in (A) and (B) are drawn according the three states in (C).

RESULTS AND DISCUSSION

Trpzip4 Beta-Hairpin Unfolds and Refolds in a Broad Force Range. To attach handles from which mechanical unfolding and refolding of a protein can be carried out along a desired direction, existing methods first get rid of all native cysteines in the protein, which is followed by mutating two specific residues to cysteines. For large proteins, it is relatively easy to identify mutations that do not disturb protein structures. However, for small peptides in which each residue is critical for structural stability, this approach becomes inappropriate. It is possible to place two cysteines at the N- and C-termini, respectively. Nevertheless, the close distance between the two cysteines in a small peptide facilitates the formation of a disulfide bond between them, making it difficult for the handle attachment. By applying a click chemistry approach,[19,32] this drawback can be avoided.

First, we respectively attached two alkyne-labeled glycine residues (see Supporting Information, Scheme S1 for the structure) to the N- and C-termini of the Trpzip4 peptide with a sequence of $G_1E_2W_3T_4W_5D_6D_7A_8T_9K_{10}T_{11}W_{12}T_{13}W_{14}T_{15}E_{16}$. The modified peptide showed a CD spectrum identical to the pure Trpzip4,[20] suggesting minimal inference from the chemical modifications (Figure S1, Supporting Information). The attachment of the two azide-labeled 2028 bp DNA handles was accomplished through the copper-catalyzed azide–alkyne cycloaddition (CuAAC) reaction.[32] The two free ends of the handles were functionalized with biotin and digoxigenin, respectively, which facilitated the assembly of the peptide–DNA hybrid between surfaces of two spherical particles (1.87 and 2.10 μm in radii) via affinity interactions (Figure 1A). After the two spheres were caught in two optical traps separately, the unfolding and refolding of Trpzip peptides were repetitively performed with a force loading rate of 5.5 pN s^{-1}. Both force and extension of molecules were recorded at 1000 Hz.

The recorded force vs extension plot (F–X curve, Figure 1B) showed two basic processes: stretching a single peptide molecule from 0 to 60 pN and relaxing the peptide to zero force in the opposite direction. For each F–X curve, we subtracted the extension of the stretching from that of the relaxing at a particular force. The resulting extension difference (Δx) was converted to the change in contour length (ΔL) as a function of force according to the worm-like-chain model (WLC).[19,37,59] Compared to traditional methods in which each contour length was obtained from WLC fitting of an F–X curve, our method adopts a completely different strategy in two folds. First, we numerically converted F–X curves to ΔL–F plots, which avoids the unidentifiability problem of the WLC model in which different sets of fitting parameters may be obtained from each F–X curve. Second, we used Δx to convert ΔL, by which tedious registration of different F–X curves (due to baseline drift for example) is not necessary.

dx.doi.org/10.1021/bi500194g | Biochemistry 2014, 53, 5978–5986

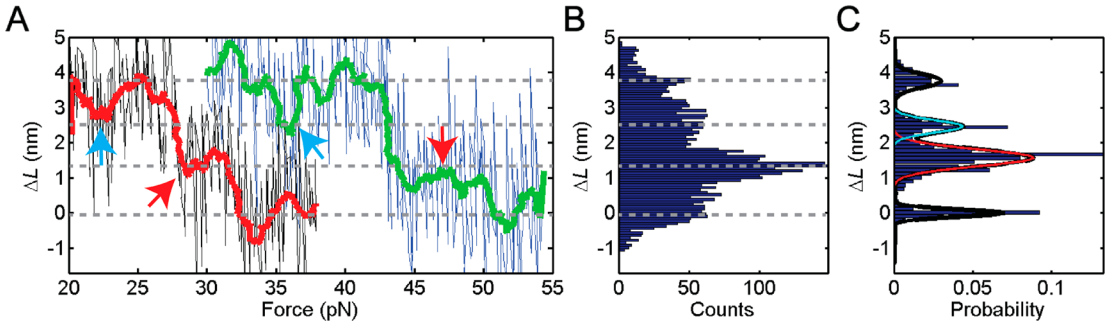

Figure 3. Unfolding and refolding of Trpzip2 beta-hairpins. (A) Two $\Delta L-F$ traces show stepwise changes of ΔL (black and blue in 100 Hz, red and green in 5 Hz filtering). Red arrows indicate the intermediate state during unfolding, while the cyan arrows indicate the intermediate state during refolding. (B) ΔL histogram of 10 traces reveals multiple populations. (C) The PoDNano analysis of 247 $\Delta L-F$ traces identifies unfolded (0 nm), folded (3.8 ± 0.2 nm), and intermediate (1.6 ± 0.2 and 2.5 ± 0.2 nm) states during unfolding and refolding of Trpzip2 beta-hairpins. Solid curves are the Gaussian fittings showing the four states. Red and cyan curves depict the intermediates during unfolding and refolding processes, respectively. Because of the unsymmetrical nature of the $\Delta L-F$ plots (see Figure S3), these two intermediates represent the same species. For comparison, dashed gray lines in (A) and (B) are drawn according different states in (C).

The $\Delta L-F$ plot allows direct visualization of peptide folding and unfolding processes (Figure 1C). For example, we observed that Trpzip4 unfolds at ~23 pN with ΔL of ~5 nm (Figure 1C, blue trace). Such a transition becomes more obvious when comparing the $\Delta L-F$ plot of a control DNA construct that does not contain any peptide sequence (Figure 1C, black trace).

The broad range of force in which transitions occur, the small magnitude of transitions (ΔL < 5 nm), and the fast transition kinetics have made it rather difficult to identify a force at which unfolding or refolding of Trpzip4 beta-hairpin takes place reversibly and discernibly (hopping) in order to retrieve transition energetics with a force clamp setting.[15,16] In fact, when we applied a constant force in the range of 15−40 pN, no obvious hopping was observed. Taking advantage of the fact that a transition of ΔL is independent of force in the $\Delta L-F$ plots, we set out to determine populations from ΔL measurements.

PoDNano Analysis Identifies Three States during Unfolding of Trpzip4 Peptide. Individual $\Delta L-F$ traces reveal that the transition of Trpzip4 beta-hairpin follows multiple pathways under mechanical tension. In addition to the two-state transition (Figure 2A, red and blue traces), we surprisingly found that this simple peptide can unfold from the native state through an intermediate state, i.e., following a three-state model (Figure 2A, yellow and cyan traces). The three-state transition becomes obvious when a ΔL histogram was constructed from the four traces (Figure 2B).

For overall population analysis, we overlapped 261 $\Delta L-F$ traces of Trpzip4 peptides (Figure S2A, Supporting Information), which accounts for a total of 113 821 data points after 100 Hz smoothing (black). The overall ΔL distribution of the Trpzip4 peptide shows a clear dependency on force (Figure S2A). Between 18 and 45 pN, the Trpzip4 undergoes from folded state (larger ΔL) to unfolded state (smaller ΔL) when the force is increased (Figure S2A, white trace for a 4 Hz filter). Data filtered with smaller bandwidth revealed more details during the unfolding and refolding processes (Figure S2A, red and black traces for 20 and 100 Hz filters, respectively). The overall ΔL histogram can be fit best by a function with three Gaussian peaks (Figure S2B, best fitting was determined by χ^2 test; see Materials and Methods). We propose the population with ΔL = 0 nm at the high force region as the unfolded Trpzip4 peptide, while the ΔL = 4.8 nm species at lower force region as folded beta-hairpin. With this assignment, we calculated contour length per amino acid as 0.35 nm (see Materials and Methods). This value is in line with the literature,[16,44,52,57] which supports our assignment. The population with $\Delta L \approx$ 2.1 nm is consistent with the intermediate identified from individual traces (Figure 2B), which corroborates the presence of the intermediate.

With respect to the small ΔL transitions (<5 nm), the Gaussian fitting comes with large uncertainties as suggested by the broad width of each peak (3.4, 5.4, and 2.1 nm). To accurately determine the ΔL of each population, we applied a statistical resampling method, bootstrapping, to pinpoint the most probable peak center through Gaussian fitting. This bootstrap strategy employs 3000 resampling groups with 113 821 data points in each group. In each resampling group, a ΔL histogram was constructed to be fitted by Gaussian equations with number of Gaussian components determined by the χ^2 test (see Materials and Methods for details). The Gaussian centers of the two largest populations were then collected to construct an overall ΔL histogram. Similar approach previously developed in our lab (Population Deconvolution at Nanometer resolution, or PoDNano[37,59]) has enabled us to differentiate species with 0.47 nm difference in ΔL. Three ΔL states were well resolved by this new PoDNano strategy (Figures 2C and S2C), with the narrow Gaussian width (0.3 nm) for all populations. Each population corresponds to the one that is identified in the Gaussian fitting of the original data set (Figure S2B). Since the algorithm selects the most probable peak centers, the final PoDnano histogram reflects the most probable populations, instead of all populations that blur the resolution. This is the reason for the increased resolution. As a control, a DNA construct without peptide shows a single population of ΔL = 0 nm after the same statistical treatment (Figure 2D), indicating no folded structure is present.

The intermediate population shows ΔL of 2.1 ± 0.2 nm (mean ± std), which is equivalent to the unfolding of eight amino acids (see Materials and Methods for calculation). Since external force was applied along the pairwise unzipping direction from the N- and C-termini, we rationalize that the unfolded eight amino acids should originally locate at the stem of the beta-hairpin as illustrated in Figure 2C. Such a conformation matches with a partial hairpin held together by the W_5 and W_{12} tryptophan pair, which is known to stabilize a structure via $\pi-\pi$ stacked indole groups.[20,60] Previously,

dx.doi.org/10.1021/bi500194g | Biochemistry 2014, 53, 5978−5986

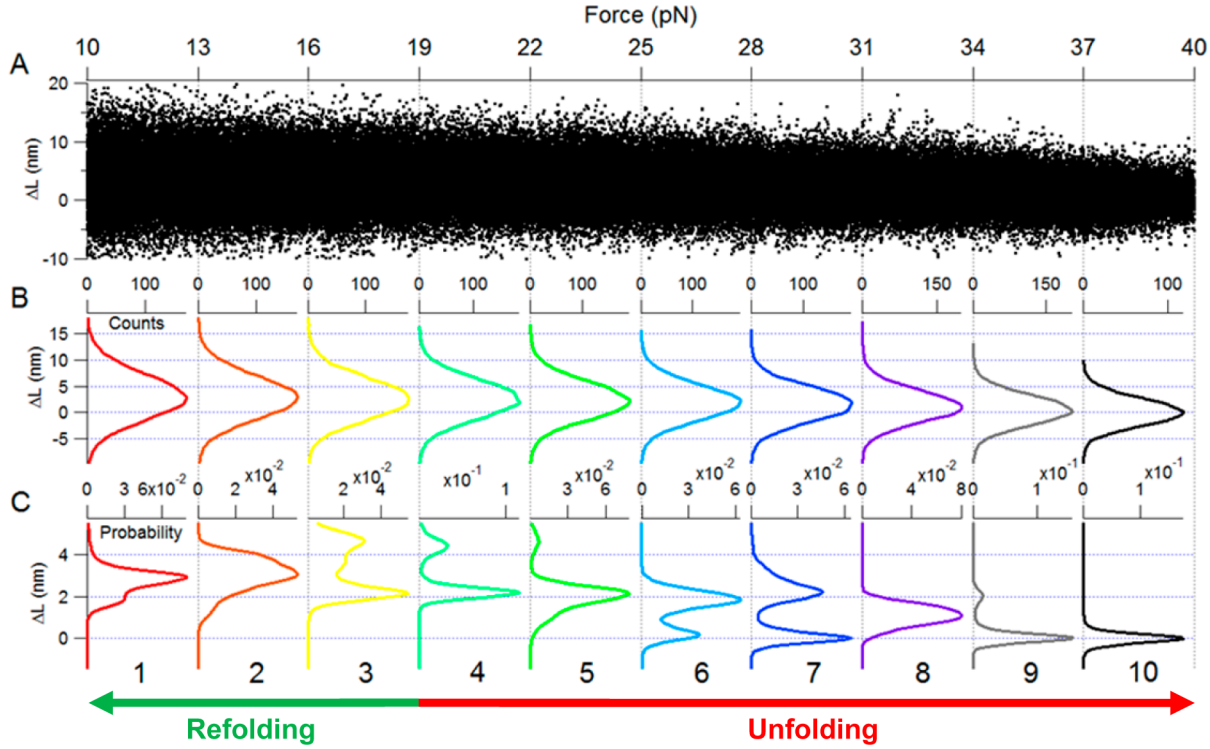

Figure 4. Population deconvolution with PSFs elaborates force-dependent folding and unfolding processes of Trpzip4. (A) 261 overlapped ΔL–F traces (same as Figure 2A) are split into 10 sections between 10 and 40 pN with 3-pN interval. (B) Histograms of ΔL for 10 force sections. (C) ΔL populations for each individual section after deconvolution with PSFs. Force sections predominated with refolding or unfolding process are approximately indicated by green or red arrows, respectively.

simulations[61] and spectroscopic experiments[62] have suggested the presence of multistates without explicit conformations during the unfolding of Trpzip peptides.

A Single Intermediate State Can Present Two ΔL Peaks for Folding and Unfolding Transitions. Because of the unsymmetrical nature of the ΔL–F plot, an intermediate that is not located halfway between a fully folded and an unfolded state may present two different ΔL values during unfolding and refolding process, respectively (see Figure S3, Supporting Information for details). The 2.1 nm intermediate revealed during unfolding should present a ∼2.8 nm ΔL population during refolding (see Figure S4, Supporting Information for calculation). Although our PoDNano strategy can resolve this 0.7 nm difference,[37,59] we did not observe the 2.8 nm ΔL population after deconvolution. We surmise that the unfolding intermediate of the Trpzip4 beta-hairpin has a longer lifetime than that during the refolding, resulting in a statistically predominant ΔL population (2.1 nm) during the unfolding. The fact that folding process usually occurs at lower force range with decreased signal-to-noise ratio may also compromise the deconvolution for the refolding intermediate.

To further explore the folding and unfolding mechanism of Trpzip β-hairpins, we mechanically unfolded Trpzip2 peptide, which contains 12 aas with a sequence of $S_1W_2T_3W_4E_5N_6$-$G_7K_8W_9T_{10}W_{11}K_{12}$. Similar to Trpzip4, two tryptophan pairs (W_2 and W_{11}; W_4, and W_9) contribute to stabilize the beta-hairpin.[20,60,63] Although the size of the Trpzip2 hairpin is even smaller than that of Trpzip4, individual ΔL–F traces showed similar stepwise features (Figure 3A, notice the dashed lines), which suggests that beta-hairpin in Trpzip2 unfolds via intermediate states as well. Similar to Trpzip4, we hypothesize that tryptophan pairs could stabilize these intermediates.

In the case of Trpzip2, we mixed 10 individual traces to construct the ΔL histogram (Figure 3B), which shows more than three populations. After population analysis based on 247 traces, two ΔL peaks of 1.6 ± 0.2 nm and 2.5 ± 0.2 nm (mean ± std) were observed clearly (Figure 3D). These two values match very well with those of a hairpin structure stabilized by the W_4 and W_9 tryptophan pair during the unfolding and refolding processes, respectively (see Figure S4 for ΔL calculation). The reason that twin peaks were resolved for the intermediate of Trpzip2, but not Trpzip4, can be attributed to the fact that Trpzip2 refolds at relatively higher force region than Trpzip4 (compare Figures 2A and 3A), which gives a higher signal-to-noise ratio for Trpzip2. In addition to these two peaks that represent the same intermediate, two other populations appeared after PoDNano analysis in Figure 3D. The ΔL = 3.8 ± 0.2 nm (mean ± std) species is consistent with a fully folded beta-hairpin, whereas the ΔL = 0 nm species corresponds to the totally unfolded state. These assignments were confirmed as contour length per amino acid (0.35 nm, see Materials and Methods) calculated from the fully folded structure (12 amino acids) matches closely with the literature (0.34–0.40 nm).[16,44,52,57]

The fact that intermediates in both Trpzip2 and Trpzip4 are stabilized by tryptophan pairs suggests a generalized folding and unfolding mechanism in which π–π stacking in the side group of amino acids stabilizes the two branches of a hairpin by serving as a button-and-hole feature. Unfolding Trpzip beta-hairpin can thus be slowed down by this feature. On the other side, refolding is facilitated because the tryptophan pair brings the rest of the hairpin together and locks the conformation. To explore these scenarios, we investigated the effect of

dx.doi.org/10.1021/bi500194g | Biochemistry 2014, 53, 5978–5986

intermediates on the unfolding and refolding transitions of Trpzip4 peptide.

Pseudo Constant Force Analysis Reveals Stepwise Unfolding and Refolding of Trpzip4 Hairpins. Force is known to tilt the free energy trajectory of unfolding or refolding of biomacromolecules.[64] To account for the force pretension, we sectioned overlapping $\Delta L-F$ traces into 3-pN intervals between 10 and 40 pN (Figure 4A). Within each section, it is reasonable to assume that the ΔL measured is equivalent to that obtained under a constant force condition ($\pm$1.5 pN).

Using this pseudo constant force analysis, we first obtained ΔL histogram for each force section (Figure 4B). We found that ΔL population gradually shifts from 4.6 to 0.0 nm when force increases (see Figure S5A for overall ΔL populations at different force segments). This trend agrees well with both individual (Figure 2A) and overall $\Delta L-F$ traces (Figure S2A) discussed above. We also observed that ΔL population becomes narrower (width decreases from 5.6 to 3.7 nm, Figure S5A) with force. This could be attributed to two reasons. First, fewer states are present in the high force region. Second, the noise in the ΔL measurement decreases with force.

The broad widths in ΔL histograms prevent accurate identification of different species and quantitation of their abundance, by which free energy transition trajectories are derived based on Boltzmann distribution.[15,16] Although we could apply our PoDNano strategy to deconvolute species, the method is not highly accurate to quantify the abundance of each species. Deconvolution using point spread function (PSF) presents a robust approach to obtain accurate population profiles.[15,16] Therefore, we obtained PSFs at different force sections after overlapping $\Delta L-F$ plots of a control molecule that contains no peptide sequence (see Materials and Methods and Figure S6, Supporting Information).

After deconvolution with these PSFs, histograms of ΔL reveal detailed transition populations (Figure 4C and Figure S5B) at each force section. First, ΔL values for folded, unfolding intermediates, and unfolded states of Trpzip4 obtained from panels in Figure 4C are in excellent agreement with aforementioned PodDNano analyses (4.6 $\pm$ 0.8, 2.1 $\pm$ 0.6, and 0 $\pm$ 0.3 nm (PSF) vs 4.8 $\pm$ 0.3, 2.1 $\pm$ 0.2 and 0 $\pm$ 0.3 nm (mean $\pm$ std, PoDNano)), firmly validating the PoDNano approach. The fully folded beta-hairpin (ΔL = 4.6 nm) decreases its population with force, while the unfolding intermediate of Trpzip4 (ΔL = 2.1 nm) becomes predominant in the 16–25 pN force range. Above 25 pN, the unfolding intermediate gradually disappears, while the fully unfolded state (ΔL = 0 nm) takes over eventually. On the other hand, below 16 pN, the unfolded species reduces its population, while the ΔL = 2.8 nm species (Figure 4C panels 1–2 and Figure S5B) increases abundance with decreasing force. Because of the unsymmetrical nature of the $\Delta L-F$ plots (Figure S3), the ΔL = 2.8 nm species during the refolding matches with the intermediate (ΔL = 2.1 nm) during the unfolding of the Trpzip4 hairpin (see Figure S4 for calculation). Interestingly, the PSF deconvolution strategy identified this intermediate (ΔL = 2.8 nm) below 19 pN (Figure S5B). Therefore, the reason that PoDNano did not resolve this species could be due to the force range in which PoDNano was applied (>19 pN). When we extended the force range to 10–40 pN, we found that two intermediate states with expected ΔL of 2.1 and 2.8 nm can now be resolved (Figure S7, Supporting Information) by the PoDNano analysis. However, the peak shape becomes complex and baseline fluctuates probably due to increased noise at lower force regions.

Taken together, these mechanical unfolding experiments provide convincing evidence for the presence of intermediates in the Trpzip2 and Trpzip4 β-hairpins. The folding and unfolding of Trpzip hairpins are faster than current temporal resolutions in high spatial resolution mechanical unfolding approaches.[65,66] However, by applying a force pretension to these peptides, we were able to tilt the unfolding/refolding energy landscape to trap intermediates in a local energy minimum.[67] This eventually allowed us to identify the intermediates using the ergodicity principle[68] with the assistance of the PoDNano analysis.

CONCLUSIONS

Using single-molecule mechanical unfolding approaches in an optical tweezers instrument, we investigated the folding mechanism of the beta-hairpin in Trpzip peptides. We identified intermediates that are likely stabilized by tryptophan pairs in both Trpzip4 and Trpzip2 peptides. The presence of the intermediate sheds light on the mechanism of how small peptides with stable secondary structures can have critical functions, which has been demonstrated, for example, in the nucleotide hydrolysis by a helicase through dynamic conversion among discrete conformations.[69]

ASSOCIATED CONTENT

Supporting Information

Scheme S1 and Figures S1–S7. This material is available free of charge via the Internet at http://pubs.acs.org.

AUTHOR INFORMATION

Corresponding Author

*E-mail: hmao@kent.edu. Phone: 330-672-9380.

Present Address

#Department of Bionanoscience, Kavli Institute of Nanoscience, Delft University of Technology, Lorentzweg 1, 2628 CJ Delft, The Netherlands.

Funding

This work was partially supported by National Science Foundation (NSF, CHE-1026532).

Notes

The authors declare no competing financial interest.

ACKNOWLEDGMENTS

We thank Deepak Koirala and Philip Yangyuoru for the preparation of the 35-nt DNA hairpins.

REFERENCES

(1) Nilsson, K. P., Lovelace, E. S., Caesar, C. E., Tynngard, N., Alewood, P. F., Johansson, H. M., Sharpe, I. A., Lewis, R. J., Daly, N. L., and Craik, D. J. (2005) Solution structure of chi-conopeptide MrIA, a modulator of the human norepinephrine transporter. *Biopolymers 80*, 815–823.

(2) Sinthuvanich, C., Veiga, A. S., Gupta, K., Gaspar, D., Blumenthal, R., and Schneider, J. P. (2012) Anticancer beta-hairpin peptides: membrane-induced folding triggers activity. *J. Am. Chem. Soc. 134*, 6210–6217.

(3) Tugarinov, V., Zvi, A., Levy, R., and Anglister, J. (1999) A cis proline turn linking two beta-hairpin strands in the solution structure of an antibody-bound HIV-1IIIB V3 peptide. *Nat. Struct. Biol. 6*, 331–335.

(4) Rosen, O., Sharon, M., Quadt-Akabayov, S. R., and Anglister, J. (2006) Molecular switch for alternative conformations of the HIV-1 V3 region: implications for phenotype conversion. *Proc. Natl. Acad. Sci. U. S. A. 103*, 13950−13955.
(5) Chetal, P., Chauhan, V. S., and Sahal, D. (2005) A Meccano set approach of joining trpzip a water soluble beta-hairpin peptide with a didehydrophenylalanine containing hydrophobic helical peptide. *J. Peptide Res. 65*, 475−484.
(6) Barthe, P., Rochette, S., Vita, C., and Roumestand, C. (2000) Synthesis and NMR solution structure of an alpha-helical hairpin stapled with two disulfide bridges. *Protein Sci. 9*, 942−955.
(7) Li, L. L., Zhang, R., Yin, L., Zheng, K., Qin, W., Selvin, P. R., and Lu, Y. (2012) Biomimetic surface engineering of lanthanide-doped upconversion nanoparticles as versatile bioprobes. *Angew. Chem., Int. Ed. Engl. 51*, 6121−6125.
(8) Jackel, C., Kast, P., and Hilvert, D. (2008) Protein design by directed evolution. *Annu. Rev. Biophys. 37*, 153−173.
(9) Thirumalai, D., O'Brien, E. P., Morrison, G., and Hyeon, C. (2010) Theoretical Perspectives on Protein Folding. *Annu. Rev. Biophys. 39*, 159−183.
(10) Berkovich, R., Hermans, R. I., Popa, I., Stirnemann, G., Garcia-Manyes, S., Berne, B. J., and Fernandez, J. M. (2012) Rate limit of protein elastic response is tether dependent. *Proc. Natl. Acad. Sci. U. S. A. 109*, 14416−14421.
(11) Maillard, R. A., Chistol, G., Sen, M., Righini, M., Tan, J., Kaiser, C. M., Hodges, C., Martin, A., and Bustamante, C. (2011) ClpX(P) generates mechanical force to unfold and translocate its protein substrates. *Cell 145*, 459−469.
(12) Glynn, S. E., Nager, A. R., Baker, T. A., and Sauer, R. T. (2012) Dynamic and static components power unfolding in topologically closed rings of a AAA+ proteolytic machine. *Nat. Struct. Mol. Biol. 19*, 616−622.
(13) Bustamante, C., Chemla, Y. R., Forde, N. R., and Izhaky, D. (2004) Mechanical processes in biochemistry. *Annu. Rev. Biochem. 73*, 705−748.
(14) Morrison, G., Hyeon, C., Hinczewski, M., and Thirumalai, D. (2011) Compaction and tensile forces determine the accuracy of folding landscape parameters from single molecule pulling experiments. *Phys. Rev. Lett. 106*, 138102.
(15) Woodside, M. T., Anthony, P. C., Behnke-Parks, W. M., Larizadeh, K., Herschlag, D., and Block, S. M. (2006) Direct Measurement of the Full, Sequence-Dependent Folding Landscape of a Nucleic Acid. *Science 314*, 1001−1004.
(16) Gebhardt, J. C., Bornschlogl, T., and Rief, M. (2010) Full distance-resolved folding energy landscape of one single protein molecule. *Proc. Natl. Acad. Sci. U. S. A. 107*, 2013−2018.
(17) Gupta, A. N., Vincent, A., Neupane, K., Yu, H., Wang, F., and Woodside, M. T. (2011) Experimental validation of free-energy-landscape reconstruction from non-equilibrium single-molecule force spectroscopy measurements. *Nat. Phys. 7*, 631−634.
(18) Liphardt, J., Onoa, B., Smith, S. B., Tinoco, I., and Bustamante, C. (2001) Reversible Unfolding of Single RNA Molecules by Mechanical Force. *Science 292*, 733−737.
(19) Yu, Z., Koirala, D., Cui, Y., Easterling, L. F., Zhao, Y., and Mao, H. (2012) Click Chemistry Assisted Single-Molecule Fingerprinting Reveals a 3D Biomolecular Folding Funnel. *J. Am. Chem. Soc. 134*, 12338−12341.
(20) Cochran, A. G., Skelton, N. J., and Starovasnik, M. A. (2001) Tryptophan zippers: stable, monomeric beta -hairpins. *Proc. Natl. Acad. Sci. U. S. A. 98*, 5578−5583.
(21) Andersen, N. H., Olsen, K. A., Fesinmeyer, R. M., Tan, X., Hudson, F. M., Eidenschink, L. A., and Farazi, S. R. (2006) Minimization and optimization of designed beta-hairpin folds. *J. Am. Chem. Soc. 128*, 6101−6110.
(22) Santiveri, C. M., and Jimenez, M. A. (2010) Tryptophan residues: scarce in proteins but strong stabilizers of beta-hairpin peptides. *Biopolymers 94*, 779−790.
(23) Munoz, V., Thompson, P. A., Hofrichter, J., and Eaton, W. A. (1997) Folding dynamics and mechanism of beta-hairpin formation. *Nature 390*, 196−199.
(24) Du, D., Zhu, Y., Huang, C. Y., and Gai, F. (2004) Understanding the key factors that control the rate of beta-hairpin folding. *Proc. Natl. Acad. Sci. U. S. A. 101*, 15915−15920.
(25) Culik, R. M., Jo, H., DeGrado, W. F., and Gai, F. (2012) Using thioamides to site-specifically interrogate the dynamics of hydrogen bond formation in beta-sheet folding. *J. Am. Chem. Soc. 134*, 8026−8029.
(26) Lewandowska, A., Oldziej, S., Liwo, A., and Scheraga, H. A. (2010) beta-hairpin-forming peptides; models of early stages of protein folding. *Biophys Chem. 151*, 1−9.
(27) Fuller, A. A., Du, D., Liu, F., Davoren, J. E., Bhabha, G., Kroon, G., Case, D. A., Dyson, H. J., Powers, E. T., Wipf, P., Gruebele, M., and Kelly, J. W. (2009) Evaluating β-turn mimics as β-sheet folding nucleators. *Proc. Natl. Acad. Sci. U. S. A. 106*, 11067−11072.
(28) Stotz, C. E., and Topp, E. M. (2004) Applications of model beta-hairpin peptides. *J. Pharm. Sci. 93*, 2881−2894.
(29) Galzitskaya, O. V., Higo, J., and Finkelstein, A. V. (2002) Alpha-helix and beta-hairpin Folding from experiment, analytical theory and molecular dynamics simulations. *Curr. Protein Peptide Sci. 3*, 191−200.
(30) Patel, D. J. (1999) Adaptive recognition in RNA complexes with peptides and protein modules. *Curr. Opin. Struct. Biol. 9*, 74−87.
(31) Theis, K., Skorvaga, M., Machius, M., Nakagawa, N., Van Houten, B., and Kisker, C. (2000) The nucleotide excision repair protein UvrB, a helicase-like enzyme with a catch. *Mutat. Res. 460*, 277−300.
(32) Kolb, H. C., Finn, M. G., and Sharpless, K. B. (2001) Click Chemistry: Diverse Chemical Function from a Few Good Reactions. *Angew. Chem., Int. Ed. 40*, 2004−2021.
(33) Du, D., Tucker, M. J., and Gai, F. (2006) Understanding the mechanism of beta-hairpin folding via phi-value analysis. *Biochemistry 45*, 2668−2678.
(34) Yu, Z., Schonhoft, J. D., Dhakal, S., Bajracharya, R., Hegde, R., Basu, S., and Mao, H. (2009) ILPR G-quadruplexes formed in seconds demonstrate high mechanical stabilities. *J. Am. Chem. Soc. 131*, 1876−1882.
(35) Koirala, D., Dhakal, S., Ashbridge, B., Sannohe, Y., Rodriguez, R., Sugiyama, H., Balasubramanian, S., and Mao, H. (2011) A single-molecule platform for investigation of interactions between G-quadruplexes and small-molecule ligands. *Nat. Chem. 3*, 782−787.
(36) Dhakal, S., Schonhoft, J. D., Koirala, D., Yu, Z., Basu, S., and Mao, H. (2010) Coexistence of an ILPR i-motif and a partially folded structure with comparable mechanical stability revealed at the single-molecule level. *J. Am. Chem. Soc. 132*, 8991−8997.
(37) Yu, Z., Gaerig, V., Cui, Y., Kang, H., Gokhale, V., Zhao, Y., Hurley, L. H., and Mao, H. (2012) The Tertiary DNA Structure in the Single-Stranded hTERT Promoter Fragment Unfolds and Refolds by Parallel Pathways via Cooperative or Sequential Events. *J. Am. Chem. Soc. 134*, 5157−5164.
(38) Smith, S. B., Cui, Y. J., and Bustamante, C. (1996) Overstretching B-DNA: The elastic response of individual double-stranded and single-stranded DNA molecules. *Science 271*, 795−799.
(39) Greenleaf, W. J., Frieda, K. L., Foster, D. A., Woodside, M. T., and Block, S. M. (2008) Direct observation of hierarchical folding in single riboswitch aptamers. *Science 319*, 630−633.
(40) Mills, J. B., Vacano, E., and Hagerman, P. J. (1999) Flexibility of Single-Stranded DNA: Use of Gapped Duplex Helices to Determine the Persistence Lengths of Poly(dT) and Poly(dA). *J. Mol. Biol. 285*, 245−257.
(41) Tinland, B., Pluen, A., Sturm, J., and Weill, G. (1997) Persistence Length of Single-Stranded DNA. *Macromolecules 30*, 5763−5765.
(42) Record, M. T. J., Anderson, C. F., and Lohman, T. M. (1978) Thermodynamic analysis of ion effects on the binding and conformational equilibria of proteins and nucleic acids: the roles of ion association or release, screening, and ion effects on water activity. *Q. Rev. Biophys. 11*, 103−178.

(43) Laurence, T. A., Kong, X., Jager, M., and Weiss, S. (2005) Probing structural heterogeneities and fluctuations of nucleic acids and denatured proteins. *Proc. Natl. Acad. Sci. U. S. A. 102*, 17348−17353.
(44) Ainavarapu, S. R., Brujic, J., Huang, H. H., Wiita, A. P., Lu, H., Li, L., Walther, K. A., Carrion-Vazquez, M., Li, H., and Fernandez, J. M. (2007) Contour length and refolding rate of a small protein controlled by engineered disulfide bonds. *Biophys. J. 92*, 225−233.
(45) Yang, G., Cecconi, C., Baase, W. A., Vetter, I. R., Breyer, W. A., Haack, J. A., Matthews, B. W., Dahlquist, F. W., and Bustamante, C. (2000) Solid-state synthesis and mechanical unfolding of polymers of T4 lysozyme. *Proc. Natl. Acad. Sci. U. S. A. 97*, 139−144.
(46) Dietz, H., and Rief, M. (2006) Protein structure by mechanical triangulation. *Proc. Natl. Acad. Sci. U. S. A. 103*, 1244−1247.
(47) Erickson, H. P. (1994) Reversible unfolding of fibronectin type III and immunoglobulin domains provides the structural basis for stretch and elasticity of titin and fibronectin. *Proc. Natl. Acad. Sci. U. S. A. 91*, 10114−10118.
(48) Trombitas, K., Greaser, M., Labeit, S., Jin, J. P., Kellermayer, M., Helmes, M., and Granzier, H. (1998) Titin extensibility in situ: entropic elasticity of permanently folded and permanently unfolded molecular segments. *J. Cell Biol. 140*, 853−859.
(49) Sarkar, A., Caamano, S., and Fernandez, J. M. (2005) The elasticity of individual titin PEVK exons measured by single molecule atomic force microscopy. *J. Biol. Chem. 280*, 6261−6264.
(50) Carrion-Vazquez, M., Marszalek, P. E., Oberhauser, A. F., and Fernandez, J. M. (1999) Atomic force microscopy captures length phenotypes in single proteins. *Proc. Natl. Acad. Sci. U. S. A. 96*, 11288−11292.
(51) Carrion-Vazquez, M., Li, H., Lu, H., Marszalek, P. E., Oberhauser, A. F., and Fernandez, J. M. (2003) The mechanical stability of ubiquitin is linkage dependent. *Nat. Struct. Biol. 10*, 738−743.
(52) Oesterhelt, F., Oesterhelt, D., Pfeiffer, M., Engel, A., Gaub, H. E., and Muller, D. J. (2000) Unfolding pathways of individual bacteriorhodopsins. *Science 288*, 143−146.
(53) Wang, M. D., Yin, H., Landick, R., Gelles, J., and Block, S. M. (1997) Stretching DNA with optical tweezers. *Biophys. J. 72*, 1335−1346.
(54) Baumann, C. G., Smith, S. B., Bloomfield, V. A., and Bustamante, C. (1997) Ionic effects on the elasticity of single DNA molecules. *Proc. Natl. Acad. Sci. U. S. A. 94*, 6185−6190.
(55) Stigler, J., Ziegler, F., Gieseke, A., Gebhardt, J. C., and Rief, M. (2011) The complex folding network of single calmodulin molecules. *Science 334*, 512−516.
(56) Gao, Y., Sirinakis, G., and Zhang, Y. (2011) Highly anisotropic stability and folding kinetics of a single coiled coil protein under mechanical tension. *J. Am. Chem. Soc. 133*, 12749−12757.
(57) Cecconi, C., Shank, E. A., Bustamante, C., and Marqusee, S. (2005) Direct observation of the three-state folding of a single protein molecule. *Science 309*, 2057−2060.
(58) Shank, E. A., Cecconi, C., Dill, J. W., Marqusee, S., and Bustamante, C. (2010) The folding cooperativity of a protein is controlled by its chain topology. *Nature 465*, 637−640.
(59) Yu, Z., and Mao, H. (2013) Non-B DNA structures show diverse conformations and complex transition kinetics comparable to RNA or proteins-a perspective from mechanical unfolding and refolding experiments. *Chem. Rec 13*, 102−116.
(60) Yang, W. Y., Pitera, J. W., Swope, W. C., and Gruebele, M. (2004) Heterogeneous folding of the trpzip hairpin: full atom simulation and experiment. *J. Mol. Biol. 336*, 241−251.
(61) Hills, R. D. J., Lu, L., and Voth, G. A. (2010) Multiscale Coarse-Graining of the Protein Energy Landscape. *PLoS Comput. Biol. 6*, e1000827.
(62) Huang, J., Li, G., Wu, Z., Song, Z., Zhou, Y., Shuai, L., Weng, X., Zhou, X., and Yang, G. (2009) Bisbenzimidazole to benzobisimidazole: from binding B-form duplex DNA to recognizing different modes of telomere G-quadruplex. *Chem. Commun. (Cambridge)*, 902−904.
(63) Snow, C. D., Qiu, L., Du, D., Gai, F., Hagen, S. J., and Pande, V. S. (2004) Trp zipper folding kinetics by molecular dynamics and temperature-jump spectroscopy. *Proc. Natl. Acad. Sci. U. S. A. 101*, 4077−4082.
(64) Evans, E. (1998) Energy landscapes of biomolecular adhesion and receptor anchoring at interfaces explored with dynamic force spectroscopy. *Faraday Discuss.*, 1−16.
(65) Moffitt, J. R., Chemla, Y. R., Izhaky, D., and Bustamante, C. (2006) Differential detection of dual traps improves the spatial resolution of optical tweezers. *Proc. Natl. Acad. Sci. U. S. A. 103*, 9006−9011.
(66) Moffitt, J. R., Chemla, Y. R., Smith, S. B., and Bustamante, C. (2008) Recent advances in optical tweezers. *Annu. Rev. Biochem. 77*, 205−228.
(67) Peng, Q., and Li, H. (2008) Atomic force microscopy reveals parallel mechanical unfolding pathways of T4 lysozyme: evidence for a kinetic partitioning mechanism. *Proc. Natl. Acad. Sci. U. S. A. 105*, 1885−1890.
(68) Hyeon, C., Morrison, G., and Thirumalai, D. (2008) Force-dependent hopping rates of RNA hairpins can be estimated from accurate measurement of the folding landscapes. *Proc. Natl. Acad. Sci. U. S. A. 105*, 9604−9609.
(69) Satapathy, A. K., Kulczyk, A. W., Ghosh, S., van Oijen, A. M., and Richardson, C. C. (2011) Coupling dTTP hydrolysis with DNA unwinding by the DNA helicase of bacteriophage T7. *J. Biol. Chem. 286*, 34468−34478.